A98-31466

ICAS-98-1,7,1

DIFFICULTIES IN THE APPLICATION OF STABILITY DERIVATIVES TO THE MANOEUVRING AERODYNAMICS OF COMBAT AIRCRAFT

D I Greenwell
Defence Evaluation and Research Agency
Bedford, UK

Abstract

The stability derivative concept is shown to have a number of theoretical and practical failings, resulting from its original purpose in permitting the linearisation and decoupling of the six degree-of-freedom equations of motion. In particular, the introduction of 'acceleration derivatives' is shown to be mathematically incorrect, and to entail an upper frequency limit on the input aircraft motion. A number of experimental difficulties in the application of the derivative model to the manoeuvring aerodynamics of combat aircraft are presented and discussed.

Introduction

The 'stability derivative' methodology for the representation of air loads in the equations of motion of aerospace vehicles is well-established, and has given good results for conventional aircraft for almost 90 years. However, the concept has a number of fundamental flaws which are becoming more and more significant for combat aircraft due both to increasing manoeuvre capabilities and to increasingly non-linear aerodynamic characteristics. As an example, the enormous scatter in lateral characteristics measured in flight presented in Figure 1 [1] for a combat aircraft manoeuvring at higher angles of attack graphically illustrates the shortcomings of the stability derivative model in this flight regime.

Although well-known to specialists in the field of manoeuvring aerodynamics, the problems in the stability derivative model are not widely appreciated. This is perhaps due to the great age and acquired respectability of the methodology, which is reinforced by the way in which it is presented in the great majority of flight dynamics text books.

In the author's experience, most aerodynamicists who do not have a strong background in flight dynamics (and conversely, most flight dynamicists who do not have a strong background in aerodynamics) react with astonishment and disbelief when the difficulties with stability derivatives are pointed out to them. The concept is such a basic element in experimental and simulation studies of both manoeuvring aerodynamics and flight dynamics that to attack it is almost unthinkable.

The purpose of this paper is to illustrate for non-specialists the shortcomings in the stability derivative concept, firstly through an examination of the flaws and limitations in the basic mathematical development, and secondly via a number of examples of wind tunnel measurements of combat aircraft dynamic characteristics. Of particular significance in the latter case is the appearance of motion frequency effects on stability derivatives measured in small-amplitude oscillatory tests.

The Stability Derivative Model

Linearised equations of motion

The failings of the stability derivative formulation can be best illustrated by examining the route by which it is derived. At the risk therefore of repeating the obvious, consider the conventional linearised equations of motion for a rigid symmetric airframe having a uniform mass distribution [2,3]:

$$\begin{aligned} \Delta X &= m\Delta\dot{u} + g\,\Delta\theta\cos\theta_0 \\ \Delta Y &= m\Delta\dot{v} + u_0\Delta r - g\,\Delta\phi\cos\theta_0 \\ \Delta Z &= m\Delta\dot{w} - u_0\Delta q + g\,\Delta\theta\sin\theta_0 \\ \Delta L &= I_x\Delta\dot{p} - I_{zx}\Delta\dot{r} \\ \Delta M &= I_y\Delta\dot{q} \\ \Delta N &= I_z\Delta\dot{r} - I_{zx}\Delta\dot{p} \end{aligned} \qquad (1)$$

where

$$\begin{aligned} \Delta\dot{\phi} &= \Delta p + \Delta r\tan\theta_0 \\ \Delta\dot{\theta} &= \Delta q \\ \Delta\dot{\psi} &= \Delta r\sec\theta_0 \end{aligned} \qquad (2)$$

The reference flight conditions are denoted by a subscript 0 and the disturbances (or perturbation quantities) by a prefix Δ. The reference condition is assumed to be symmetric and with no angular velocity, so that $v_0 = p_0 = q_0 = r_0 = \phi_0 = 0$, whilst working in stability axes gives $w_0 = 0$.

In order to solve these equations analytically it is necessary to introduce expressions for the disturbance forces and moments ΔX etc. Consider the equations of

motion rearranged as a set of first-order differential equations

$$\dot{\mathbf{x}}(t) = \mathbf{A}\,\mathbf{x}(t) + \mathbf{B}\,\eta(t) \qquad (3)$$

where x is the state vector $[\Delta u, \Delta v, \ldots \Delta\psi]$, η the input or control vector, **A** the state matrix and **B** the input matrix. **A** and **B** have constant elements and are derived from equations (4) and (5). However, in order to do this, the expressions for the disturbance forces and moments must be in a consistent form, that is as a further set of first-order linear differential equations in the perturbation variables.

It is this requirement that results in the application of the stability derivative concept, but it is also at this point that a basic flaw in the concept appears. Fundamentally, equations (1) and (2) relate the *response* (the vehicle motion) of a linear physical system (the linearised equations of motion) to the *input* (the applied aerodynamic loads). On the other hand, in the case of the vehicle aerodynamic characteristics the vehicle motion is the *input* and the aerodynamic loads the *response*.

Quasi-steady aerodynamic loads

The introduction of a consistent formulation for the aerodynamic disturbance forces is handled very differently by authors of flight dynamics textbooks. The commonest approach is simply to state without justification that the aerodynamic forces behave linearly with any perturbation quantity, thus for example [4,5,6,7]

$$\Delta X = \frac{\partial X}{\partial u}\Delta u + .. + \frac{\partial X}{\partial \alpha}\Delta w + \frac{\partial X}{\partial \dot{w}}\Delta \dot{w} + .. \frac{\partial X}{\partial p}\Delta p + \ldots \qquad (4)$$

where the partial derivatives $\partial X/\partial u$ etc are constants known as 'stability' or 'aerodynamic' derivatives. Note the inclusion of 'acceleration' derivatives with respect to the first derivatives of the perturbation variables. Substitution of expressions of the form of (4) in equations (1) then permits a straightforward algebraic manipulation to give the state-variable form of equation (3).

In other texts, an attempt is made to give a more formal justification for equation (4), ranging from a simple statement that it results from a Taylor series expansion in the perturbation variables [8] to a more detailed description of the expansion and subsequent truncation [2,3,9,10]. For example, Reference 3 treats equation (4) as the sum of a number of Taylor series expansions in the perturbation quantities *and their derivatives*:

$$\begin{aligned}\Delta X = &\left(\frac{\partial X}{\partial u}\Delta u + \frac{\partial^2 X}{\partial u^2}\frac{(\Delta u)^2}{2!} + \ldots\right) \\ &+ \left(\frac{\partial X}{\partial v}\Delta v + \frac{\partial^2 X}{\partial v^2}\frac{(\Delta v)^2}{2!} + \ldots\right) \\ &+ \ldots\ldots \\ &+ \left(\frac{\partial X}{\partial \dot{u}}\Delta \dot{u} + \frac{\partial^2 X}{\partial \dot{u}^2}\frac{(\Delta \dot{u})^2}{2!} + \ldots\right)\end{aligned} \qquad (5)$$

and so on, with additional series terms in the higher order derivatives.

Since the motion variables are small, the series are truncated to the first order terms only, whilst only the first derivatives are retained. References 2 and 9 more "correctly" use a multi-variable Taylor series, thus introducing additional cross terms in the expansion which are then neglected along with the rest of the higher order terms later.

References 2 and 10 are unusual, in justifying the inclusion of higher order derivatives in the series expansion by means of an initial expansion in time rather than in the perturbation variables. In this case, the aerodynamic loads at time t are expressed as a functional of the entire past history of the state variables, so that for example

$$X(t) = X\left[\alpha(\tau)\right] \qquad -\infty \le \tau \le t \qquad (6)$$

When $\alpha(\tau)$ can be expressed as a Taylor series

$$\alpha(\tau) = \alpha(t) + (\tau - t)\dot{\alpha}(t) + \frac{(\tau - t)^2\ddot{\alpha}(t)}{2} + \ldots \qquad (7)$$

then equation (6) becomes

$$X(t) = X\left(\alpha(t), \dot{\alpha}(t), \ddot{\alpha}(t), \ldots\right) \qquad (8)$$

from which a further series expansion of the right-hand side yields equation (5). A similar procedure is followed in Reference 10.

It must be emphasised at this point that the preceding derivation of a mathematical model for the disturbance air loads was undertaken for one reason, and for one reason only - namely to linearise the equations of motion, *not* the aerodynamic characteristics.

Limits of applicability

Unfortunately, equation (4) and subsequent expansions contain a fundamental flaw, in the introduction of additional partial derivatives with respect to the rates of change of perturbation quantities, ie $\dot{u}$, $\dot{v}$ and $\dot{w}$. This is mathematically incorrect, since these are *not* independent variables [11]. An alternative statement can be found in Reference 10, in which it is noted that the expansion of equation (8) is based on the assumption that in the definition of (for example) the aerodynamic derivative

$$X_{\dot{\alpha}} = \lim_{\Delta\dot{\alpha}\to 0}\frac{\Delta X}{\Delta\dot{\alpha}} \qquad (9)$$

the limit on the right-hand side exists - an assumption which is then demonstrated to be untenable in at least one simple case.

These 'higher order' terms were not present in Bryan's original formulation of the stability derivative concept [12]; their subsequent inclusion was the result of ad-hoc attempts to represent the influence of the motion time history whilst maintaining a form consistent with the linearised equations of motion, and as such was a

reasonably successful approach for conventional aircraft and conventional manoeuvres [2,13]. Unfortunately, these 'acceleration' derivatives have acquired respectability with age, and become entrenched to the point where many flight dynamicists and aerodynamicists are simply unaware of their limitations.

The question then arises: what are the limitations of the stability derivative model?

There are a number of ways of looking at this, from the empirical to the analytical. Empirically, a limit to the applicability of the stability derivative formulation appears when one measure aerodynamic characteristics (in flight or in the wind tunnel) which cannot be adequately represented by it. Figure 1 is an example of such a case from the in-flight determination of lateral derivatives; examples from wind tunnel experiments will be examined later in this paper.

Analytically, one can compare the model with more sophisticated methods - and in this case it turns out that in order to demonstrate the limitations 'more sophisticated' need be no more than a simple linear (*not* 'linearised') aerodynamic model [14].

Hancock [15] gives an elegant exposition which retains the acceleration derivative but adds a residual error term, by considering the response of a linear aerodynamic system to a unit step input at time τ, ie

$$\begin{aligned} \alpha(t) = H(t-\tau) &= 0, \quad t < \tau \\ &= 1, \quad t \geq \tau \end{aligned} \tag{10a}$$

The lift coefficient response is

$$C_L(t) = a_0 f_H(t-\tau) \tag{10b}$$

where a_0 is the steady-state lift curve slope and $f_H(t)$ the step (or indicial) response function. The significance of the assumption of linearity is that the step response $f_H(t-\tau)$ is independent of the past motion history and of the step size. For an arbitrary input $\alpha(t)$ starting from zero incidence, the output is given by the convolution integral [15,16]

$$C_L(t) = a_0 \int_0^t f_H(t-\tau)\frac{d\alpha}{d\tau}\,d\tau \tag{11}$$

which can be expanded [15] as

$$\begin{aligned} C_L(t) = a_0 \Bigg[\alpha(t) &- \frac{d\alpha}{d\tau}\int_0^t \left(1 - f_H(t-\tau)\right)d\tau \\ &+ \frac{d\alpha}{d\tau}\int_0^t \left(1 - f_H(t-\tau)\right)\left(1 - \frac{\frac{d\alpha}{d\tau}(\tau)}{\frac{d\alpha}{dt}(t)}\right)d\tau \Bigg] \end{aligned} \tag{12}$$

The first integral is constant and a function of the step response f_H. The second is a time-varying term which is a function of the input motion $\alpha(t)$. Equation (12) can therefore be rewritten as

$$C_L(t) = a_0\,\alpha(t) - \left[a_0 k_H + \textit{residual term}(t)\right]\dot{\alpha}(t) \tag{13}$$

which is equivalent to

$$\begin{aligned} C_{L\alpha} &= \frac{\partial C_L}{\partial \alpha} = a_0 \\ C_{L\dot{\alpha}} &= \frac{\partial C_L}{\partial \dot{\alpha}} = -a_0 k_H \end{aligned} \tag{14}$$

Equations (13) and (14) gives rise to a number of observations:

a) there are no "higher order" derivative terms.

b) the acceleration derivative is directly related to the steady-state derivative, and generally of opposite sign.

c) the acceleration derivative would be more accurately described as an 'integral' term.

d) the validity of the stability derivative formulation depends on the magnitude of the residual error term, which in turn depends on the form of the step response and on the motion time history.

An alternative approach is given by Etkin [17], who considers the response of a linear system using the Laplace Transform methodology from classical control theory [18]. Again assuming for simplicity an input starting from zero incidence, an 'aerodynamic transfer function' (Figure 2a for example) is defined as

$$\bar{C}_L(s) = G_{L\alpha}(s)\bar{\alpha}(s) \tag{15}$$

where the over-bar indicates the Laplace Transform of the function and s is the Laplace variable. The use of stability derivatives implies an approximation to the transfer function $G_{L\alpha}$ in the form of a power series in s, since

$$C_L(t) = C_{L\alpha}\,\alpha(t) + C_{L\dot{\alpha}}\,\dot{\alpha}(t)$$

is equivalent to

$$\bar{C}_L(s) = \left[C_{L\alpha} + C_{L\dot{\alpha}}\,s\right]\bar{\alpha}(s) \tag{16}$$

In order to assess the validity of this approximation, it is noted that the step or indicial linear aerodynamic response in lift can be adequately represented by a sum of exponential terms [17,19], that is

$$f_H(t) = a_0 + a_1\delta(t) + a_2 e^{b_2 t} + a_3 e^{b_3 t} + \ldots \tag{17}$$

where the impulse term $\delta(t)$ represents the 'added mass' effect. The corresponding transfer function is

$$\begin{aligned} G_{L\alpha}(s) &= s\bar{f}_H(s) \\ &= a_0 + a_1 s + a_2\frac{s}{s-b_2} + a_3\frac{s}{s-b_3} + \ldots \end{aligned} \tag{18}$$

from which the overwhelming temptation is to expand the exponential terms as power series of the form

$$\frac{s}{s-b} = -\frac{s}{b}\left(1 - \frac{s}{b}\right)^{-1} = -\frac{s}{b}\left(1 + \frac{s}{b} + \frac{s^2}{b^2} + \ldots\right) \tag{19}$$

and then neglect higher order terms to give a transfer function of the form of equation (16). Unfortunately, the power series expansion diverges for $|s/b| > 1$, and hence is valid only for values of s inside the circle of convergence $|s| = |b|$, Figure 3.

To give physical significance to this limit, note that the frequency response of a linear system transfer function can be determined by substitution of $i\omega$ for s [18], in which case the range of validity for a power series expansion of equation (18) becomes

$$\omega_{input} < b_{\min} \tag{20}$$

where b_{min} is the lowest natural frequency in the exponential response contributions to the step response function in equation (17).

An immediate observation is that the frequency limit precludes step or impulse input functions, since these have a very wide frequency content (indeed, an infinitely wide frequency content in the case of a pure impulse). Unfortunately, in the form of control doublets these motions are the theoretical and practical basis of in-flight identification of aircraft stability characteristics!

Equation (20) indicates why the stability derivative model has been so successful for conventional aircraft and manoeuvres. Typical attached configuration flows have non-dimensional time constants which are typically less than 0.5 - 1, giving an upper limit on non-dimensional motion frequency of 1-2. Such high values translate into transient manoeuvre rates which have until recently been beyond the capabilities of conventional aircraft.

However, whilst combat aircraft manoeuvre capabilities have been increasing steadily in recent years, we are also seeing the signature-driven reappearance of highly swept planforms with high incidence aerodynamics dominated by extensive areas of separated flows and by the formation of leading-edge vortices. The non-dimensional time constants associated with leading-edge vortices, particularly in the presence of vortex bursting, can be very large - typically between 5 and 25. The corresponding upper input frequency bounds of 0.04 to 0.2 are well within current and future manoeuvre envelopes and therefore result in severe difficulties with the stability derivative model. It should also be noted that even within the range of validity of the expansion, as characteristic motion frequencies are increased the additional errors introduced by the truncation to first order will become large.

Motion Frequency Effects

Typical experimental characteristics

Having demonstrated a range of theoretical objections to the stability derivative formulations, some practical manifestations will now be considered, first and foremost of which is the appearance of motion frequency effects in the experimental measurement of the derivatives using small-amplitude oscillations. As far as the stability derivative model is concerned, the frequency should have no effect on the derivatives; however, this is not always the case as Figure 4 shows for a 60° delta wing (replotted from Reference 20). A strong motion frequency dependency in both lateral and longitudinal dynamic derivatives is not uncommon, and has been reported on many occasions.

The general behaviour of the rolling moment due to sideslip derivatives in Figure 4 as frequency is reduced is particularly significant, with the 'in-phase' static derivative $C_{l\beta}$ approaching the steady-state value whilst the 'in-quadrature' acceleration derivative $C_{l\dot{\beta}}$ approaches a large negative value. Similar trends have been reported for dynamic yawing [21], rolling [22], and pitching [23] derivatives of basic delta wings, and of representative combat aircraft configurations [24,25].

In the past, common practice has been to ignore the frequency effects (when measured) and to use data for an oscillation frequency felt to be most representative of practical aircraft manoeuvres. This has often resulted in a number of different aerodynamic models being developed for a given aircraft, each optimised for a particular flight regime or manoeuvre.

Frequency effects for linear characteristics

Although incompatible with the simple stability derivative model, the effects of motion frequency are quite consistent with a linear system response [13].

For example, consider the measurement of the rolling moment derivatives due to sideslip

$$C_{l\beta} = \frac{\partial C_l}{\partial \beta}, \quad C_{l\dot{\beta}} = \frac{\partial C_l}{\partial\left(\dot{\beta} b/2U\right)} \tag{21}$$

during small-amplitude sinusoidal lateral (swaying) oscillations

$$\begin{aligned} \beta(t) &\approx \frac{\dot{y}(t)}{U} = \beta_0 \sin(\omega t) \\ \dot{\beta}(t) &\approx \frac{\ddot{y}(t)}{U} = \beta_0 \omega \cos(\omega t) \end{aligned} \tag{22}$$

The restriction to "small" amplitudes permits the assumption that the rolling moment response is linear, and hence can be written as

$$C_l(t) = A\sin(\omega t) + B\cos(\omega t) \tag{23}$$

The rolling moment derivatives are then determined from the 'in-phase' and 'in-quadrature' components of the rolling moment response

$$\begin{aligned} C_{l\beta} &= \frac{A}{\beta_0} \\ C_{l\dot{\beta}} &= \frac{B}{\beta_0(\omega b/2U)} = \frac{B}{\beta_0 \Omega} \end{aligned} \tag{24}$$

An alternative means of expressing the aerodynamic response equation (22) is as

$$C_l(t) = \left(C_{l\beta,0}\,\beta_0\right) AR\sin(\omega t + \phi)$$

or in terms of non-dimensional frequency and time

$$C_l(\tau) = \left(C_{l\beta,0}\,\beta_0\right) AR\sin(\Omega\tau + \phi) \tag{25}$$

where AR and ϕ are the frequency dependent amplitude ratio and phase lag of the aerodynamic transfer function

and $C_{l\beta 0}$ the steady-state gain, Figure 2a. The amplitude ratio and phase lag are

$$AR(\Omega) = \frac{\sqrt{C_{l\beta,\omega}{}^2 + C_{l\dot{\beta},\omega}{}^2 \Omega^2}}{C_{l\beta,0}}$$
$$\phi(\Omega) = \tan^{-1}\left(\frac{C_{l\dot{\beta},\omega}\,\Omega}{C_{l\beta,\omega}}\right) \qquad (26)$$

or conversely,

$$C_{l\beta,\omega} = C_{l\beta,0}\, AR\cos(\phi)$$
$$C_{l\dot{\beta},\omega} = \frac{C_{l\beta,0}\, AR\sin(\phi)}{\Omega} \qquad (27)$$

A good model for the rolling moment response is obtained by dividing it into two separate components [14,26]:

a) an attached flow contribution with gain $C_{l\beta,att}$, which has effectively zero time lag and

b) a separated flow contribution which for a simple configuration is approximated by a first-order lag with gain $C_{l\beta,sep}$ and non-dimensional time constant τ_{sep}.

The resulting aerodynamic transfer function (Figure 2b) in terms of the non-dimensional Laplace variable $\hat{s}$ is

$$\overline{C}_{l\beta}(\hat{s}) = C_{l\beta,att} + \frac{C_{l\beta,sep}}{1 + \tau_{sep}\,\hat{s}} \qquad (28)$$

From equation (28) the frequency dependent derivatives are

$$C_{l\beta,\omega} = C_{l\beta,att} + C_{l\beta,sep}\frac{1}{1+\left(\Omega\tau_{sep}\right)^2}$$
$$C_{l\dot{\beta},\omega} = C_{l\beta,sep}\frac{-\tau_{sep}}{1+\left(\Omega\tau_{sep}\right)^2} \qquad (29a)$$

and therefore

$$C_{l\dot{\beta},\omega} = -\tau_{sep}\left(C_{l\beta,\omega} - C_{l\beta,att}\right) \qquad (29b)$$

from which the steady-state derivatives are

$$C_{l\beta,0} = C_{l\beta,att} + C_{l\beta,sep}$$
$$C_{l\dot{\beta},0} = -\tau_{sep} C_{l\beta,0} \qquad (29c)$$

Equation (29a) gives a good fit to the typical experimental frequency characteristics shown in Figure 4, whilst equation (29b) suggests that a cross-plot of acceleration vs static derivatives should give a straight line with a slope of $-\tau_{sep}$ and an extrapolated x-axis intercept at $C_{l\beta,att}$.

Figure 5 shows that for a simple delta wing this is indeed the case, while Figure 6 shows that the extrapolated 'attached flow' gains $C_{l\beta,att}$ lie on the trend established by the steady-state measurements at lower incidences. The 'separated flow' time constants τ_{sep} derived from Figure 5 are negligible at low incidence, but start to increase rapidly at around 12° incidence (as the vortex burst comes on to the wing) up to a peak at around 32° (where the vortex burst reaches the wing apex).

Comparing equation (29c) with (14), it can be seen that the response time constant $-\tau_{sep}$ is equivalent to Hancock's step response integral k_H [15].

Motion Amplitude Effects

Another aspect of experimental dynamic wind tunnel testing that causes problems with the stability derivative formulation are the often significant effects of motion amplitude. Although this is a non-linear effect, it can occur when the basic steady-state characteristics appear linear, and/or even when the motion amplitudes are so small that linearity would seem to be assured.

For example, Figure 7 [27] shows a very strong effect of yaw amplitude between $\psi_0 = \pm 2°$ and $\pm 4°$, even though the corresponding steady-state characteristics are apparently reasonably linear in this range. Reference 28 shows similar effects for oscillation amplitudes down to $\psi_0 = \pm 0.76°$. There are two factors which can contribute to this behaviour - firstly that non-linearities in the steady-state characteristics are highly localised, and secondly that there are a number of contributors to the characteristics with differing degrees of non-linearity and dynamic response times.

The first is typical of highly swept delta wings, and also of combat aircraft configurations with strong forebody vortices (particularly when coupled with closely spaced twin fins) - Figure 8. Such localised non-linearities can lead to chaotic aircraft motion [29]. The second is typical of lower sweep angle delta wings, where for example the rolling moment response has three components - a stabilising linear attached flow contribution, a stabilising and reasonably linear leading-edge vortex flow contribution and a destabilising and highly non-linear vortex breakdown contribution. The first two contributions have relatively short time-scales, while the third is very slow to respond; in dynamic testing, therefore, the balance between the three can change very rapidly.

Amplitude effects of this nature are a particular problem for translational motion tests (ie pure sideslip or heave), where the mechanical motion amplitude is fixed and hence from equation (22) aerodynamic amplitude increases with oscillation frequency. The result can be a discontinuity in the variation of the measured dynamic derivatives with frequency as the motion amplitude crosses a critical value (Figure 9), or simply an uncertainty as to whether the trends observed are due to changes in frequency or amplitude.

Acceleration Effects

Rotary acceleration derivatives

The previous discussions have centred on translational motions for measurements of dynamic derivatives; however, most oscillatory wind tunnel test mechanisms

generate rotary motions which result in the measurement of 'combined' derivatives, for example the in-phase and in-quadrature pitching derivatives

$$C^*_{z\alpha} = C_{z\alpha} - \Omega^2 C_{z\dot{q}}$$
$$C^*_{zq} = C_{zq} + C_{z\dot{\alpha}} \qquad (30)$$

In general, the rotary acceleration terms are ignored, on the assumptions that (a) they're likely to be small and (b) the Ω^2 factor makes their contribution to the combined derivative small.

Unfortunately, once again this is no longer justifiable for combat aircraft configurations in the manoeuvring flight regime. Figure 10 illustrates this with results from small-amplitude oscillatory tests of a generic combat aircraft configuration at DERA Bedford. At high angles of attack, the effect of the yawing acceleration term $C_{l\dot{r}}$ can be seen to be large.

Direct measurements of pure angular derivatives are rare, requiring a complex 'snaking' motion mechanism for oscillations in body axes, or a rolling-flow tunnel. One exception is an unusual experiment reported in Reference 22, in which a 60° delta wing was oscillated in roll about the wind axis - ie oscillatory coning motion. Continuous motion coning tests are commonly used to measure rate derivatives - however to the author's knowledge this is the only reported instance of a 'small-amplitude' oscillatory coning experiment. (What is often referred to in the literature as 'oscillatory coning' is in fact continuous rolling motion with the roll axis inclined to the velocity vector). Figure 11 [22] shows similar frequency effects on the in-phase and in-quadrature derivatives to those described earlier for sideslipping motion, indicating a similar form of time-dependent response, with the rolling moment lagging the roll rate by a frequency-dependent phase angle ϕ.

Stability calculations also reported in Reference 22 showed a significant effect of inclusion of the roll acceleration terms in the equations of motion, particularly on the damping of the roll subsidence mode.

Convective time lags

Acceleration derivatives are generally assumed to result from convective time lags - for example between wing and tailplane. In this case it is conventionally stated that the downwash at the tail is dependent primarily on the wing trailing vortices in the vicinity of the tail and that therefore a change in circulation at the wing will take a time $\Delta t = l_t / U$ to reach the tail - Figure 12. With some manipulation, the result is a constant acceleration derivative, for example

$$C_{z\dot{\alpha}} \approx 2 V_H C_{z\alpha\, tail} \frac{d\varepsilon}{d\alpha} \qquad (31)$$

where ε is the downwash angle at the tail. This is of course a gross over-simplification, ignoring the effects both of the spanwise 'starting vortex' shed from the trailing-edge of the wing whenever the circulation changes (shown as a dashed line in Figure 12), and of the increased trailing vortex strength upstream of the tail. Reference 15 is unusual in the text books available to the author in acknowledging this fact.

The true lag effects at the tail will depend strongly on both the motion frequency and the wing/tail geometry. At low frequencies the effects of the trailing vortices dominate and the conventional model gives a reasonable approximation. At higher frequencies (of the order of the inverse of the convective time lag), the influence of the upwash from the shed 'starting' vortex begins to dominate and the acceleration derivative changes sign from positive to negative [15]. Increasing frequency still further results in the acceleration derivative falling to zero, as observed experimentally in Figure 13 (for $\alpha <$ 20°).

Virtual or 'added' inertias

However, there is another contribution which once again is generally ignored, namely the potential flow 'added mass' or 'virtual inertia' effect. In wind tunnel testing, this effect is usually said to be small and is zeroed out as part of the usual process of subtraction of 'wind-off' dynamic tares. It is possible to retain the virtual inertia contribution by either doing wind-off zeros in a vacuum, or with the model enclosed, but this is rarely done. As a phenomenon associated with low-speed, incompressible flows, the magnitude of the virtual inertia falls off rapidly as Mach Number is increased [16] so that failure to measure it is not generally a significant problem.

However, this is predicated on the assumption that the virtual inertia does not vary between 'wind-off' and 'wind-on' conditions, which is the case for low-incidence attached flows. However, there are indications that for highly swept wings at higher incidences (with the onset of flow separations and the formation of leading-edge vortices), this is not the case.

First of all, an estimate of the magnitude of the virtual inertia terms can be derived from a consideration of the contribution to the lift response to heave motion. Data on the virtual inertias of wing planforms is scarce, since the effect is primarily seen in hydrodynamics. For a 2D flat-plate aerofoil, the virtual inertia is that of a fluid cylinder enclosing the aerofoil [30] and for a 3D ellipsoid roughly half the inertia of the displaced fluid [31].

An indication of the magnitude of the virtual inertia for a 3D slender wing is given by

$$m_{virtual} = \tfrac{8}{3} \rho a^3 \qquad (32)$$

for a circular disk [31], where $m_{virtual}$ is the virtual inertia or acceleration response to motion normal to the surface, and a is the disk radius. The normal force response becomes

$$\Delta Z = m_{virtual} \dot{w} = \tfrac{8}{3} \rho a^3 \dot{w} \qquad (33a)$$

which when non-dimensionalised as equation (22) gives a constant value (independent of motion frequency) for the corresponding acceleration derivative of

$$\left(C_{z\dot{\alpha}}\right)_{virtual} = \frac{\Delta C_z}{\Delta\dot{\alpha}\bar{c}/2U} = 2 \qquad (33b)$$

A sphere would give a value of $\pi/2$ for the derivative and a 2D aerofoil a value of π.

This estimate can be compared with the measured heave derivatives (with the virtual inertia zeroed-out) shown in Figure 13a for a generic combat aircraft configuration. In this case the estimated virtual inertia term is of a similar magnitude to the lift-induced contribution at low incidences, but much smaller at higher incidences - certainly not negligible!

It should be emphasised that the magnitude of the virtual inertia contribution to the acceleration derivative is independent of relative fluid/model density - in other words, the *aerodynamic* significance of virtual inertia effects is as great in a wind tunnel experiment as it would be in a water tunnel.

As an aside, Figure 13a shows another difficulty with dynamic testing at high incidence, with a discontinuity in the steady-state characteristics resulting in a hysteresis loop in the dynamic characteristics.

Looking now at the motion frequency effects for the same aircraft, Figure 13b shows that at low incidences the acceleration derivative approaches zero as frequency is increased, consistent with the linear system response of equations (24) and (27). However, at higher incidences the derivatives appear to approach a constant positive value, indicating the presence of a true (additional) acceleration dependent component in the response. Similar behaviour is shown by the acceleration derivatives in sideslip for this configuration. One possibility is that this is the result of a increase in the virtual inertia contribution once the leading-edge vortex structure forms.

In this case the 'attached flow' structure of Figure 14a which led to equations (32) and hence (33) has been replaced by the 'separated flow structure' of Figure 14b, with two leading-edge vortices with associated feeding shear layers above the wing. The virtual inertia for a 2D flat plate can be determined from the potential jump across the plate, since from the unsteady Bernoulli equation the force per unit length due to an acceleration normal to the plate is [32]

$$\frac{\Delta L}{\Delta x} = \rho\frac{\partial}{\partial t}\int_{-a}^{a}\Delta\Phi\,dy = \frac{d\left(w\,m_{virtual}\right)}{dt} \qquad (34)$$

The potential jump $\Delta\Phi$ is directly proportional to the normal velocity component w, and so the virtual inertia $m_{virtual}$ is a constant. The formation of a leading-edge vortex pair will result in an increment in the potential function jump across the surface, and hence in the virtual inertia. The increment will depend on the strength of the vortices and on their position relative to the wing [33]. Given the equivalence between the cross-flow virtual inertia and wing lift curve slope for slender wings in attached flows [32], it appears likely that the increment in virtual inertia due to flow separation will behave in a similar manner to the vortex lift increment on these wings, increasing non-linearly with angle of attack and sweep angle.

Direct measurements of virtual inertia effects at high incidence are rare, but an indication of their magnitude can be extracted from a phenomenon that has attracted much experimental attention, namely limit cycle wing rock of 80° delta wings. Reference [34] observes that the widely varying oscillation frequencies observed in wind tunnel investigations can be correlated with wing inertia on the assumption of a constant quasi-linear aerodynamic stiffness. The equation of motion in roll is

$$I\ddot{\phi} + k\phi = 0$$

where k is the (aerodynamic) stiffness $C_{l_\phi}qSb$ and I is the wing moment of inertia. The frequency of the motion is thus given by

$$n = \frac{fc}{U} = \frac{c}{U}\sqrt{\frac{k}{I}} = \left(\frac{\sqrt{C_{l_\phi}}}{8\pi}\right)\cdot\left(\sqrt{\frac{\rho Sbc^2}{I_{wing}}}\right) = A.N_{wing} \qquad (35)$$

where A is a constant and N_{wing} a non-dimensional inertia parameter. Using an experimentally measured value for C_{l_ϕ} of 0.2, equation (35) was shown to fit a wide range of published wing rock data for 80° delta wings at an incidence of 30° (inertia parameters from 0.5 to 4). In order to examine the behaviour of the correlation at higher inertia parameters, a series of tests were then undertaken in a water channel (giving values from 7 to 35).

However, as Figure 15 shows, the measured frequencies diverge rapidly from the straight-line trend. Reference 34 speculated that this may be due to increasingly non-linear aerodynamic characteristics as frequency increases, or to the low Reynolds Numbers in the water tunnel experiments. The latter is possible, but is generally not thought to be significant for separated flows over highly swept delta wings; the former is unlikely, since non-linear effects would tend to reduce in significance as frequency is increased (see Figure 4 for example). What is more likely to be occurring is that the virtual inertia is becoming more and more significant as the relative wing inertia is reduced (and hence inertia parameter increased).

In the same way that the virtual inertias in translation are proportional to the mass of the fluid volume swept by the wing, the virtual inertia in roll is related to the moment of inertia of the swept volume. For a delta wing of span b and root chord c, the virtual inertia will be

$$I_{virtual} \propto I_{cone} = B\frac{\pi}{160}\rho b^4 c \qquad (36a)$$

where B is a constant. Equation (36a) corresponds to a *constant* inertia parameter for an 80° delta wing of

$$N_{virtual} = \sqrt{\frac{\rho S b c^2}{I_{virtual}}} = \frac{4.31}{\sqrt{B}} \qquad (36b)$$

A rough estimate for the inertia factor B for attached flow can be derived from a result in reference [30] for a 2D flat-plate aerofoil pitching about its midchord

$$I_{virtual} = \frac{\pi \rho a^4}{8}$$

which is equivalent to

$$I_{virtual} \approx \frac{\pi}{640} \rho b^4 c \qquad (37)$$

for a rolling slender delta wing, and hence $B_{attached} = 0.25$.

Substituting (36) into equation (35) gives

$$n = A \frac{N_{wing} N_{virtual}}{\sqrt{N_{wing}^2 + N_{virtual}^2}} \qquad (38)$$

which gives an excellent fit to the water tunnel data in Figure 15, with an inertia parameter $N_{virtual}$ of 9.48 and hence a factor B on the 'fluid inertia' of 1.23 - a five-fold increase on the estimate made on the basis of attached flow!

Because the virtual inertia is an incompressible flow phenomenon, the possible presence of an additional vortex lift induced component in low-speed wind tunnel measurements will need to be taken into account when extrapolating to higher (subsonic) Mach Numbers. Virtual inertias are also of particular significance for free motion testing in water tunnels, and must be taken into account when resolving aerodynamic loads from model motions [35].

Summary and Conclusions

The stability derivative concept has been shown to have a number of theoretical and practical failings, resulting from its original purpose in permitting the linearisation and decoupling of the six degree-of-freedom equations of motion. In particular, the introduction of 'acceleration derivatives' has been shown to be mathematically incorrect, and to entail an upper frequency limit on the input aircraft motion.

Experimentally, measurements of the dynamic derivatives for combat aircraft configurations display features which are inconsistent with the stability derivative concept, namely the appearance of large motion frequency and amplitude effects in derivatives measured during nominally 'small-amplitude' oscillatory motion.

Finally, it has also been shown that the normally neglected angular acceleration effects can be significant for combat aircraft configurations, both in the form of a phase lag in the response to angular velocity and in the appearance of an increment in virtual inertia due to the presence of a leading-edge vortex system.

List of Symbols

a	radius, lift curve slope, coefficients in transfer function
A,B	in-phase and in-quadrature response, coefficients in wing rock correlation
b	wing span, natural frequencies in transfer function
c	wing chord
f	frequency, Hz
g	acceleration due to gravity
$G(s)$	transfer function
$H(t)$	unit step function
I	moment of inertia
k	aerodynamic stiffness
L,M,N	applied aerodynamic moments
m	aircraft mass
n	non-dimensional frequency, fc/U
N	inertia parameter, $\sqrt{\rho S b c^2 / I}$
q	dynamic pressure, $\frac{1}{2}\rho U^2$
p, q, r	angular velocity components
s	Laplace transform variable
S	planform area
t	time
u, v, w	translational velocity components
U	freestream velocity
x, y, z	cartesian coordinates
X, Y, Z	applied aerodynamic forces
α,β	angle of attack and sideslip
ψ,Θ,ϕ	Euler attitude angles
ϕ	phase lag angle
$\delta(t)$	unit impulse
ρ	fluid density
τ	running variable in time, non-dimensional time
ω	frequency, rads^{-1}
Ω	non-dimensional frequency
Φ	potential function
$C_{l\beta}$	'static' rolling moment derivative
$C_{l\dot{\beta}}$	'dynamic' rolling moment derivative

References

1. Iliff, K.W. and Wang, K.C., 'Extraction of Lateral-Directional Stability and Control Derivatives for the Basic F-18 Aircraft at High Angles of Attack', NASA TM-4786, 1997

2. Etkin, B. and Reid, L.D., *'Dynamics of Flight: Stability and Control'*, John Wiley & Sons Inc, New York, 1996

3. Cook, M.V., *'Flight Dynamics Principles'*, Arnold, London, 1997

4. McCormick, B.W., *'Aerodynamics, Aeronautics, and Flight Mechanics'*, John Wiley & Sons Inc, New York, 1995

5. Babister, A.W., *'Aircraft Dynamic Stability and Response'*, Pergamon Press, Oxford, 1980

6. Abramson, N., *'An Introduction to the Dynamics of Airplanes'*, Dover Publications Inc, New York, 1971

7. Dickinson, B., *'Aircraft Stability and Control for Pilots and Engineers'*, Pitman & Sons Ltd, London, 1968

8. Nelson, R.C., *'Flight Stability and Automatic Control'*, McGraw-Hill, Boston, 1998

9. Seckel, E., *'Stability and Control of Airplanes and Helicopters'*, Academic Press, New York, 1964

10. Robinson, A. and Laurmann, J.A., *'Wing Theory'*, Cambridge University Press, Cambridge, 1956

11. Tobak, M. and Schiff, L.B., 'Aerodynamic Mathematical Modelling - Basic Concepts', in AGARD LS-114, 'Dynamic Stability Parameters', March 1981

12. Bryan, G.H., *'Stability in Aviation'*, MacMillan and Co, London, 1911

13. Anon., *'Introduction to Aerodynamic Derivatives, Equations of Motion and Stability'*, ESDU item 86021, 1987

14. Greenwell, D.I., 'Frequency Effects on Dynamic Stability Derivatives Obtained from Small-Amplitude Oscillatory Testing', Journal of Aircraft, to be published

15. Hancock, G.J., *'An Introduction to the Flight Dynamics of Rigid Aeroplanes'*, Ellis Horwood, New York, 1995

16. Bisplinghoff, R.L., Ashley, H. and Halfman, R.L., *'Aeroelasticity'*, Addison-Wesley Co Inc, Cambridge, 1955

17. Etkin, B., 'Aerodynamic Transfer Functions: an Improvement on Stability Derivatives for Unsteady Flight', UTIA report 42, Institute of Aerophysics, University of Toronto, October 1956

18. Atkinson, P., *'Feedback Control Theory for Engineers'*, Heineman Educational Books Ltd, London, 1972

19. Dowell, E.H., 'A Simple Method for Converting Frequency-Domain Aerodynamics to the Time Domain', NASA TM 81844, 1980

20. Lichtenstein, J.H. and Williams, J.L., 'Effect of Frequency of Sideslipping Motion on the Lateral Stability Derivatives of a Typical Delta-Wing Airplane', NACA RM L57F07, September 1957

21. Campbell, J.P., Johnson, J.L. and Hewes, D.E., 'Low-Speed Study of the Effect of Frequency on the Stability Derivatives of Wings Oscillating in Yaw with Particular Reference to High Angle-of-Attack Conditions', NACA RM L55H05, November 1955

22. Fisher, L.R., 'Experimental Determination of the Effects of Frequency and Amplitude of Oscillation on the Roll-Stability Derivatives for a 60° Delta-Wing Airplane', NASA TN D-232, March 1960

23. Khrabrov, A.H., Kolinko, K.A., Miatov, O. and Zhuk, A.H., 'Experimental Investigation of Wings Unsteady Aerodynamic Characteristics at Flow Separation Regimes', TsAGI Preprint 86, 1997

24. Grafton,S.B. and Anglin, E.L., 'Dynamic Stability Derivatives at Angles of Attack from -5° to 90° for a Variable-Sweep Fighter Configuration with Twin Vertical Tails', NASA TN D-6909, October 1972

25. Klein, V., Murphy, P.C., Curry, T.J. and Brandon, J.M., 'Analysis of Wind Tunnel Longitudinal Static and Oscillatory Data of the F-16XL Aircraft', NASA TM-97-206276, December 1997

26. Coe, P.L., Graham, A.B. and Chambers, J.R., 'Summary of Information on Low-Speed Lateral-Directional Derivatives Due to Rate of Change of Sideslip', NASA TN D-7972, September 1975

27. Fisher, L.R., 'Experimental determination of Effects of Frequency and Amplitude on the Lateral Stability Derivatives for a Delta, a Swept and an Unswept Wing Oscillating in Yaw', NACA R 1357, 1958

28. Letko, W. and Fletcher, H.S., 'Effects of Frequency and Amplitude on the Yawing Derivatives of Triangular, Swept and Unswept Wings and of a Triangular-Wing Fuselage Combination Performing Sinusoidal Yawing Oscillations', NACA TN 4390, September 1958

29. Goman, M., Khrabrov, A. and Studnev, A., 'Stochastic Self-Induced Roll Oscillations of Slender Delta Wing at High Angles of Attack', AIAA-92-4498, 1992

30. Sedov, L.I., *'Two-Dimensional Problems in Hydrodynamics and Aerodynamics'*, John Wiley & Sons Inc, 1965

31. Batchelor, G.K., *'An Introduction to Fluid Dynamics'*, Cambridge University Press, Cambridge, 1967

32. Katz, J. and Plotkin, Allen, *'Low-Speed Aerodynamics'*, McGraw-Hill Inc, New York, 1991

33. Coe, P.L., 'Stationary Vortices Behind a Flat Plate Normal to the Freestream in Incompressible Flow', AIAA Journal, Vol 10 No 1, December 1972, p1701

34. Mabey, D.G., 'Similitude Relations for Buffet and Wing Rock on Delta Wings', Progress in Aerospace Sciences, Vol 33, 1997, pp481-511

35. Nelson, M.D., 'An Experimental Investigation of Leading Edge Vortical Flow About a Delta Wing During Wing Rock', MSc Thesis, Texas A&M University, December 1991

Figures

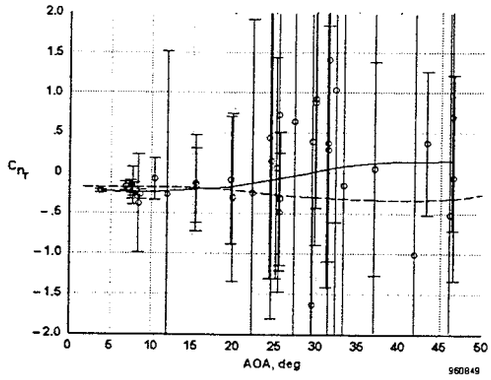

Figure 1 Scatter in lateral derivatives estimated from F-18 flight tests at high angles of attack [1]

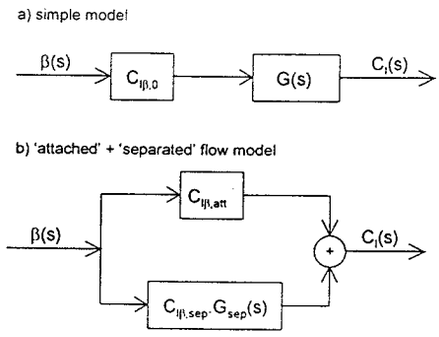

Figure 2 Aerodynamic transfer functions for rolling moment response to sideslip

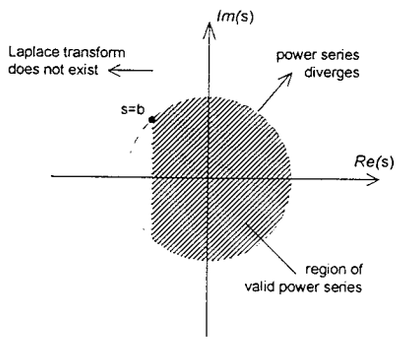

Figure 3 Region of validity of power series expansion of aerodynamic transfer function [17]

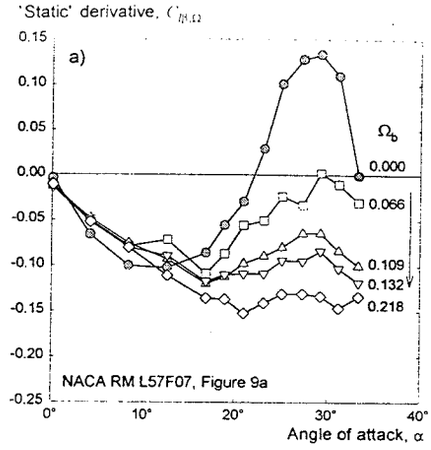

Figure 4 Effect of frequency on rolling moment due to sideslip derivatives of a 60° delta wing [20]

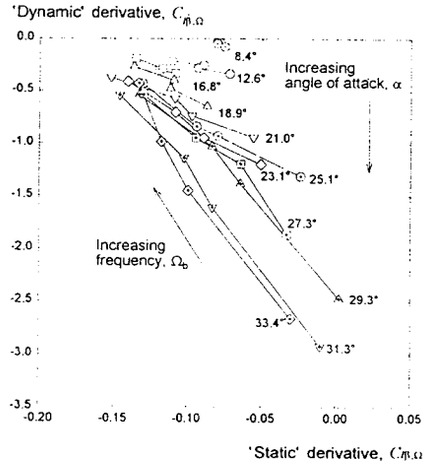

Figure 5 Cross-plot of in-phase and in-quadrature rolling moment derivatives for a 60° delta wing

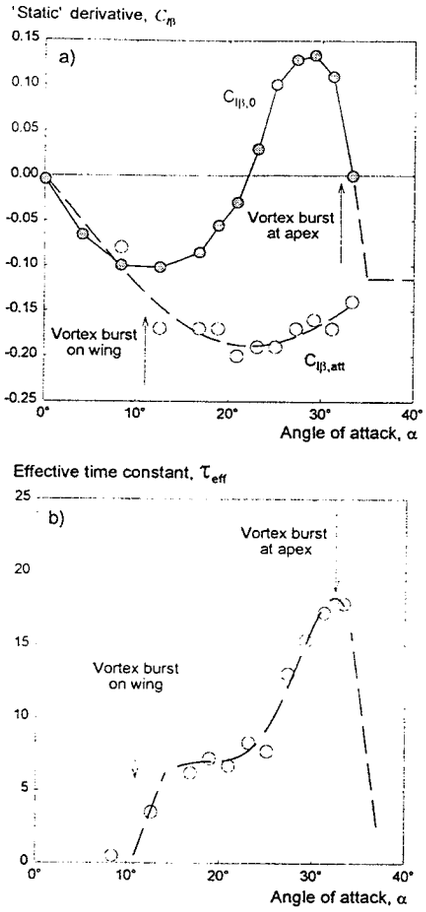

Figure 6 Aerodynamic transfer function parameters derived from derivative cross-plot

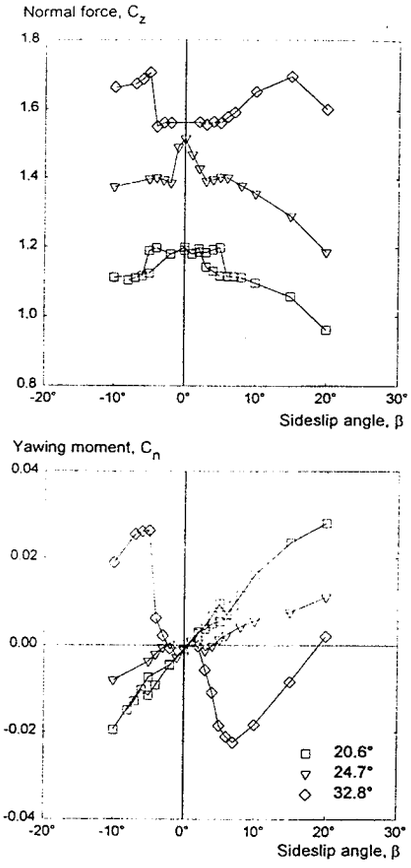

Figure 8 Localised non-linearities in combat aircraft steady-state lateral characteristics

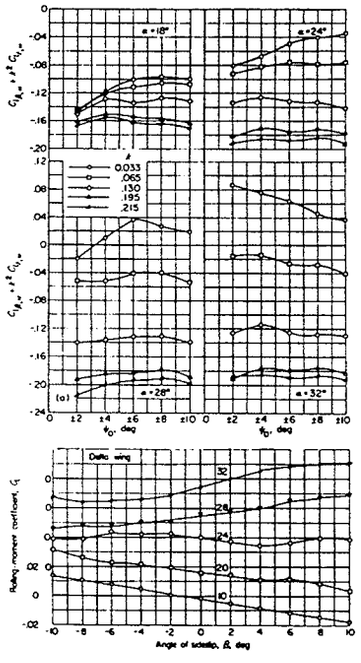

Figure 7 Effect of oscillation amplitude on rolling moment due to yaw derivatives of a 60° delta wing [27]

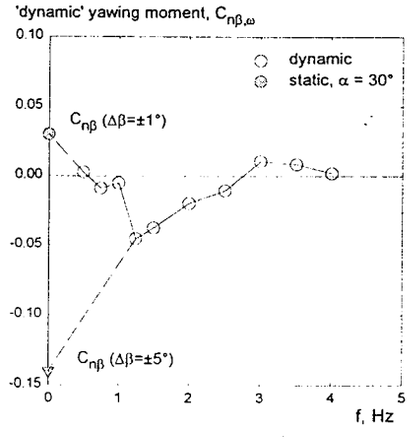

Figure 9 Amplitude effect in lateral derivatives measured in translational motion

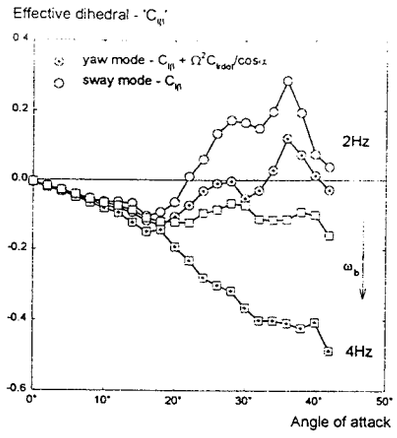

Figure 10 'Effective dihedral' measured in yawing and sideslipping motion for a generic combat aircraft configuration

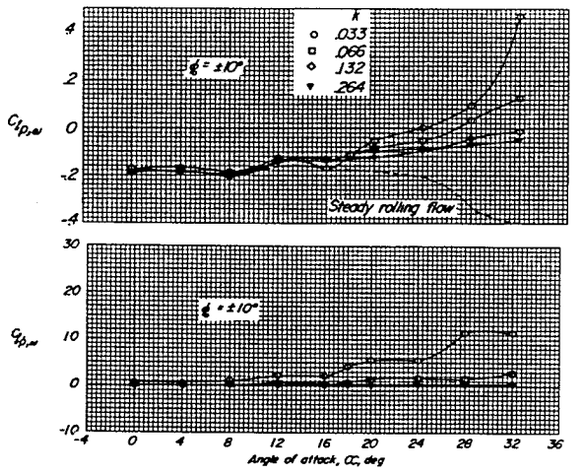

Figure 11 Effect of frequency on rolling moment derivatives due to roll rate for a 60° delta wing [22]

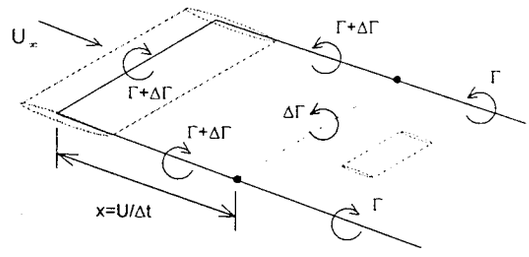

Figure 12 Conventional 'convective time lag' explanation for longitudinal acceleration derivatives

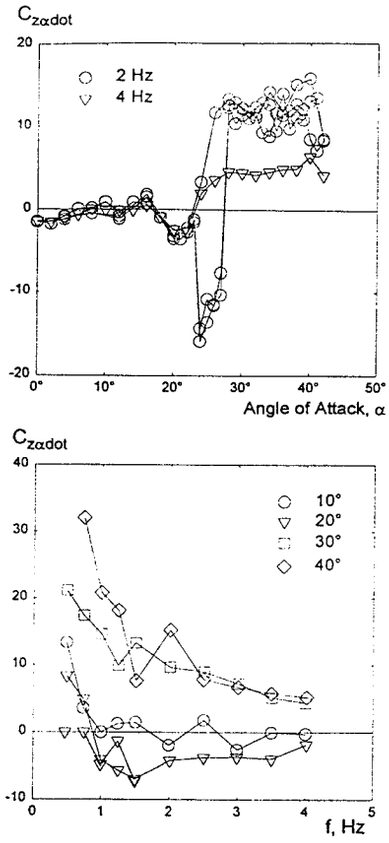

Figure 13 Acceleration response in heave for a generic combat aircraft configuration

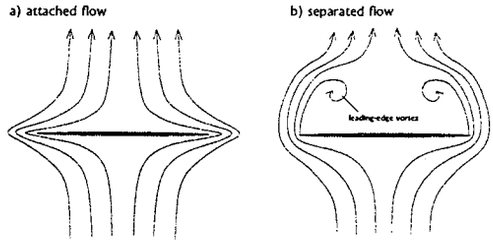

Figure 14 Sketch of attached and separated slender-wing cross-flow

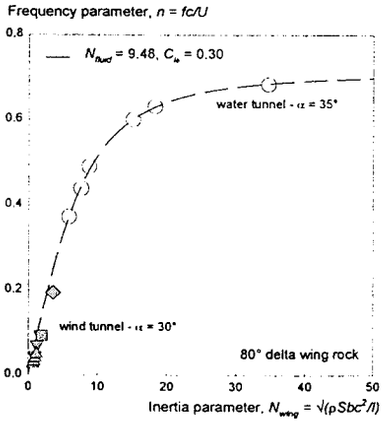

Figure 15 Variation of wing rock frequency with wing inertia parameter [34]